

Relativistic effects on the Fukui function

Nick Sablon · Remigius Mastalerz ·
Frank De Proft · Paul Geerlings · Markus Reiher

Received: 30 September 2009 / Accepted: 15 December 2009 / Published online: 8 January 2010
© Springer-Verlag 2010

Abstract The extent of relativistic effects on the Fukui function, which describes local reactivity trends within conceptual density functional theory (DFT), and frontier orbital densities has been analysed on the basis of three benchmark molecules containing the heavy elements: Au, Pb, and Bi. Various approximate relativistic approaches have been tested and compared with the four-component fully relativistic reference. Scalar relativistic effects, as described by the scalar zeroth-order regular approximation methodology and effective core potential calculations, already provide a large part of the relativistic corrections. Inclusion of spin-orbit coupling effects improves the results, especially for the heavy *p*-block compounds. We thus expect that future conceptual DFT-based reactivity studies on heavy-element molecules can rely on one of the approximate relativistic methodologies.

Keywords Relativistic quantum chemistry · Conceptual DFT · Fukui function · Heavy-element compounds

1 Introduction

A framework for the stability and reactivity interpretation of molecules and solids is provided by conceptual or chemical density functional theory (DFT) [1–6]. It is based on the general characteristics of the individual systems, thus without explicit reference to the possible partner reagents. Various milestone concepts that extended chemical reactivity theory in the middle of the past century have been unified within conceptual DFT. The importance of Hinze and Jaffé's studies on the Mulliken electronegativity [7–12], Pearson's theory on hard and soft acids and bases [13–15], and the frontier molecular orbital concepts [16, 17] as introduced by Fukui has thus been re-emphasised [18–21].

Theoretical studies on the reactivity of heavy-element compounds have been gaining more and more interest due to their increasing application in catalytic processes [22]. An accurate evaluation of the reactivity descriptors for these systems should rigorously include relativistic effects. So far, only a single study has focused on the relativistic contributions in the calculation of global reactivity indices of some group 16 compounds [23]. We propose to systematically analyse the relativistic effects as described by various (quasi-)relativistic Hamiltonians on the Fukui functions, which are used to describe the local electrophilic and nucleophilic reactivities of molecular regions within conceptual DFT. Three benchmark molecules will be analysed: $(CH_3)_2SAuCl$, $PbCl_2$, and Bi_2H_4 . These systems are prototypes for molecules involved in organometallic

Dedicated to the memory of Professor Jürgen Hinze and published as part of the Hinze Memorial Issue.

N. Sablon: Aspirant of the Research Foundation-Flanders (aspirant van het Fonds Wetenschappelijk Onderzoek-Vlaanderen).

N. Sablon, F. De Proft, and P. Geerlings are members of the QCMM Ghent-Brussels Alliance Group.

N. Sablon (✉) · F. De Proft · P. Geerlings
Eenheid Algemene Chemie, Vrije Universiteit Brussel,
Pleinlaan 2, 1050 Brussels, Belgium
e-mail: nick.sablon@vub.ac.be

R. Mastalerz · M. Reiher (✉)
Laboratorium für Physikalische Chemie, ETH Zurich,
Wolfgang-Pauli-Strasse 10, 8093 Zurich, Switzerland
e-mail: markus.reiher@phys.chem.ethz.ch

chemistry and especially in various carbon–carbon bond formation reactions [22]. They are associated with a broad range of reaction types such as substitution reactions, Grignard reactions, and additions to double bonds. They all contain a sixth period element, for which significant relativistic contributions are expected, and span heavy transition metal as well as *p*-block compounds.

In Sect. 2, the basics of conceptual DFT are revisited and the relativistic approximations used are briefly explained. Section 3 presents the methodology and the computational characteristics, while the results and their detailed analysis are expounded on in Sect. 4. Some final remarks are made in Sect. 5.

2 Theoretical background

2.1 Conceptual DFT

Based on a Taylor series expansion of the electronic energy E of a chemical system as a function of its number of electrons N and as a functional of its external potential $v(\mathbf{r})$, which is just the electron–nuclear potential for isolated atoms and molecules, various descriptors characterising its inherent chemical behaviour have been identified with the first and higher order (functional) derivatives of E [4]:

$$\begin{aligned} E[v(\mathbf{r}) + \Delta v(\mathbf{r}), N + \Delta N] &= E[v(\mathbf{r}), N] + \Delta N \left(\frac{\partial E}{\partial N} \right)_{v(\mathbf{r})} \\ &+ \frac{1}{2} (\Delta N)^2 \left(\frac{\partial^2 E}{\partial N^2} \right)_{v(\mathbf{r})} + \cdots + \int \left(\frac{\delta E}{\delta v(\mathbf{r})} \right)_N \Delta v(\mathbf{r}) d\mathbf{r} \\ &+ \cdots + \Delta N \int \left(\frac{\delta \partial E}{\delta v(\mathbf{r}) \partial N} \right) \Delta v(\mathbf{r}) d\mathbf{r} + \cdots \end{aligned} \quad (1)$$

The first derivative with respect to N corresponds to the electronic chemical potential μ , which equals the negative of the electronegativity, the second one has been identified as the chemical hardness η , the first functional derivative with respect to $v(\mathbf{r})$ is equal to the electron density $\rho(\mathbf{r})$, and the mixed derivative has been called the Fukui function $f(\mathbf{r})$. Depending on the kind of reagent towards which one would like to describe the reactivity of the molecule under scrutiny, the use of certain DFT indices is preferred over others. If the reagent has, for example, a high chemical hardness, the charge transfer during the reaction, and hence ΔN , will remain close to zero. The molecular regioselectivity will thus be dominated by the electron density, or on electrostatic grounds, rather than by the Fukui function, which, on the other hand, will play a decisive role when soft interactions come into play. An extensive discussion on this interpretation can be found in Ref. [4]. A large number of other, derived indices has been proposed, a discussion of which is outside the scope of this paper [3].

As already mentioned, the Fukui functions,

$$f^\pm(\mathbf{r}) = \left(\frac{\delta \partial E}{\delta v(\mathbf{r}) \partial N} \right)^\pm = \left(\frac{\delta \mu^\pm}{\delta v(\mathbf{r})} \right)_N = \left(\frac{\partial \rho(\mathbf{r})}{\partial N} \right)^\pm_{v(\mathbf{r})}, \quad (2)$$

describe the regioselective behaviour of a molecule involved in a soft, or orbital-controlled, reaction. The necessity of defining right and left side derivatives stems from the integer discontinuity in the derivatives of the electronic energy E with respect to N , as proven within a zero-temperature grand canonical ensemble framework by Perdew et al. [24]. All such derivatives in Eq. 1 should thus be provided with this indication. The right side Fukui function, $f^+(\mathbf{r})$, corresponding to an electron increase, describes the local reactivity towards nucleophilic attacks, while the left side one, $f^-(\mathbf{r})$, corresponding to an electron decrease, deals with the electrophilic attacks.

2.2 Relativistic approximations

Although we will use relativistic DFT calculations throughout this paper, we will not focus on the intricacies of the relativistic four-component Kohn–Sham model [25–28], but restrict ourselves to a brief description of the relativistic Hamiltonians used, which encompasses the most relevant theoretical background for our purposes. An elaborate exposition of relativistic quantum theory can, for example, be found in Refs. [29, 30]. The Dirac–Coulomb Hamiltonian H_{DC} ,

$$H_{DC} = \sum_{i=1}^N h_D(i) + \sum_{i=1}^N \sum_{j>i}^N \frac{1}{r_{ij}}, \quad (3)$$

where r_{ij} stands for the distance between two electrons i and j , is based on Dirac's theory of the electron and is generally considered a fully relativistic reference. The four-component one-electron Dirac operator $h_D(i)$ can in standard notation be written in Hartree atomic units (a.u.) as

$$h_D(i) = c\boldsymbol{\alpha} \cdot \mathbf{p}_i + (\beta - 1)c^2 - \sum_{A=1}^M \frac{Z_A}{R_{iA}}, \quad (4)$$

where c denotes the speed of light in vacuum (137.0359998 a.u.), $\boldsymbol{\alpha}$ a three-vector whose components are (4×4) matrices made up from Pauli spin matrices $\sigma = (\sigma_x, \sigma_y, \sigma_z)$ on the off-diagonal, and \mathbf{p}_i the linear momentum operator. The second term in Eq. 4 contains the diagonal (4×4) matrix β with $(1, 1, -1, -1)$ as elements on the diagonal and a shift in the energy by the rest energy c^2 (in atomic units) in order to match the non-relativistic energy scale. The Coulomb attraction between the electrons and the nuclei A is finally accounted for by the last term in Eq. 4.

The one-electron functions ϕ_i to be used in the single Slater determinant of a Hartree–Fock or Kohn–Sham theory consist, as a consequence of the structure of the Dirac

operator, of four components and are called molecular spinors:

$$\phi_i = \begin{pmatrix} \phi_i^1 \\ \phi_i^2 \\ \phi_i^3 \\ \phi_i^4 \end{pmatrix} = \begin{pmatrix} \phi_i^L \\ \phi_i^S \end{pmatrix}. \quad (5)$$

The large and small two-component spinors ϕ_i^L and ϕ_i^S can be obtained from one-particle eigenvalue equations, which we choose to write as:

$$(V - \varepsilon_i)\phi_i^L + c\boldsymbol{\sigma} \cdot \mathbf{p}_i \phi_i^S = 0 \quad (6)$$

$$c\boldsymbol{\sigma} \cdot \mathbf{p}_i \phi_i^L + (V - 2c^2 - \varepsilon_i)\phi_i^S = 0, \quad (7)$$

with the potential energy V comprising the sum of the electron–electron and electron–nuclei interactions (note that we assumed for the sake of brevity that all scalar potential energy operators entering V are diagonal).

Since four-component methods are computationally demanding, schemes have been developed to decouple the large and small components in the Dirac–Coulomb Hamiltonian in order to obtain an, approximate, two-component description [30]. There exist two classes of techniques: the first one is based on a unitary transformation of the Dirac–Coulomb Hamiltonian. We just mention the Foldy–Wouthuysen [31] and Douglas–Kroll–Hess [32–34] theories without going into details. The second class uses an elimination technique, of which the zeroth-order regular approximation (ZORA) [35–37] is the most popular representative, which will be applied in this study. The basic idea is to solve Eq. 7 for ϕ_i^S :

$$\phi_i^S = X(\varepsilon_i)\phi_i^L, \quad (8)$$

with the operator $X(\varepsilon_i)$ given by

$$X(\varepsilon_i) = \frac{c\boldsymbol{\sigma} \cdot \mathbf{p}_i}{(\varepsilon_i - V + 2c^2)}, \quad (9)$$

and to insert this result into Eq. 6 which gives an energy-dependent expression for the Hamiltonian that is expanded in a Taylor series to eventually yield the two-component one-electron ZORA Hamiltonian h_{ZORA} :

$$h_{\text{ZORA}}(i) = \boldsymbol{\sigma} \cdot \mathbf{p}_i \frac{c^2}{2c^2 - V} \boldsymbol{\sigma} \cdot \mathbf{p}_i + V. \quad (10)$$

Calculations can be performed with ZORA in its scalar relativistic scheme or with the inclusion of spin–orbit coupling contributions.

A final approach we will make use of is within a non-relativistic framework, including relativistic effects by means of effective core potentials (ECPs). These surrogate potentials replace the inner atomic shells and are designed to represent the relativistic effects of the core electrons by adjusting their parameters in atomic relativistic reference

calculations. Some reviews on ECPs and their applications can, for example, be found in Refs. [38, 39].

3 Methodology and computational details

It has been shown that the Fukui functions are given by finite difference formulae [19, 21]:

$$f^-(\mathbf{r}) = \rho_N(\mathbf{r}) - \rho_{N-1}(\mathbf{r}) \quad (11)$$

$$f^+(\mathbf{r}) = \rho_{N+1}(\mathbf{r}) - \rho_N(\mathbf{r}), \quad (12)$$

where $\rho_N(\mathbf{r})$, $\rho_{N-1}(\mathbf{r})$ and $\rho_{N+1}(\mathbf{r})$, respectively, denote the electron densities of the neutral, cationic and anionic systems, all at the geometry of the neutral system as the last derivative in Eq. 2 is to be evaluated at constant external potential. Even though these relations are from a strict point of view only exactly applicable within an exact theory, they are the common approach when approximate quantum chemical calculations, for example, DFT calculations with an approximate exchange–correlation functional, are performed. This is because of their proven reliability and their ease of use [3]; methods aiming at an immediate evaluation of the (functional) derivatives in Eq. 2 have been thought up [40–44], but are computationally more demanding than formulae 11 and 12.

As mentioned in Sect. 1, three representative molecules have been chosen to analyse the magnitude of the relativistic effects: $(\text{CH}_3)_2\text{SAuCl}$, PbCl_2 and Bi_2H_4 (with C_s , C_2 , and C_{2h} point group symmetries, respectively). We have calculated their neutral, cationic, and anionic electron densities on the basis of the theoretical methods introduced in Sect. 2.2 and within the non-relativistic framework for comparison. This study can be seen as a continuation of the work of some of the present authors where the relativistic effects on the topology of the electron density was systematically analysed [45].

All calculations are of the DFT type using the BP86 functional to include exchange and correlation effects [46, 47]. The geometries of the neutral molecules have been optimised at the scalar relativistic ZORA level of theory as implemented in the ADF program package [48] employing the large QZ4P all electron basis set of Slater-type functions. All the subsequent relativistic and non-relativistic calculations have been done on this geometry to ensure that the observed variations in the Fukui functions are not due to geometric changes.

The four-component calculations have been performed with the Dirac electronic structure program [49]. As large component basis sets for the heavy elements, we used the triple-zeta Gauss-type ones devised by Dyall [50, 51] in a completely decontracted way, so that all the exponents are used to construct primitive functions. This results in a

(29s, 24p, 15d, 11f, 4g, 1h) basis set size for Au, a (31s, 27p, 20d, 15f, 1g) one for Pb, and a (31s, 27p, 20d, 15f, 1g) one for Bi. These extensive sets should be close to the basis set limit. For the lighter elements, we have opted for Dunning's cc-pVTZ basis set [52], again employed in a decontracted manner. The small component basis sets have been generated by the Dirac program itself on the basis of the kinetic balance condition.

The scalar relativistic ZORA and spin-orbit relativistic ZORA calculations, as well as the non-relativistic ones have been done with the ADF package. In analogy with the geometry optimisation calculations, the QZ4P basis sets, as available in the basis set library, have been applied.

We finally used the Gaussian 03 program [53] for performing the ECP calculations. The energy consistent multi-configuration Dirac–Fock (MDF) Stuttgart–Dresden pseudopotentials [54, 55] have been chosen to replace the core electrons of the heavy-element atoms. These ECPs have been fitted to four-component numerical multi-configuration Dirac–Hartree–Fock data so that all relativistic effects (scalar and averaged spin-orbit) of the core on the retained valence part are implicitly taken into account. The contribution of the valence spin-orbit coupling effects, which can only be recovered via two-component calculations, is neglected as we formally work within a non-relativistic framework. The small-core 60MDF pseudo-potentials, replacing a [Kr]4d¹⁰4f¹⁴ core and leaving the shells with principal quantum number 5 and 6 for explicit description, have been chosen for Au, Pb, and Bi [54, 55]. The corresponding basis sets have been used while the lighter elements have been provided with Dunning's cc-pVTZ basis set.

4 Results and discussion

The calculated Fukui functions are visualised in Figs. 1, 2, and 3 as contour plots given in the molecular plane that provides most of the reactivity information. The non-relativistic Fukui functions $f_{\text{nr}}^{\pm}(\mathbf{r})$ are depicted first, followed by difference plots where the variation of the Fukui functions obtained by one of the above-mentioned methods with respect to the non-relativistic case is shown. These difference Fukui functions $\Delta f^{\pm}(\mathbf{r})$ are thus given by

$$\Delta f^{\pm}(\mathbf{r}) = f_{\text{rel}}^{\pm}(\mathbf{r}) - f_{\text{nr}}^{\pm}(\mathbf{r}), \quad (13)$$

with $f_{\text{rel}}^{\pm}(\mathbf{r})$ representing one of the (quasi-)relativistic functions. In addition, the densities of the highest occupied and lowest unoccupied molecular orbitals/spinors, $\rho_{\text{HOMO}}(\mathbf{r})$ and $\rho_{\text{LUMO}}(\mathbf{r})$, have been calculated as they can be seen as approximations to the Fukui functions within a frozen orbital approach:

$$f^-(\mathbf{r}) \approx \rho_{\text{HOMO}}(\mathbf{r}) \quad (14)$$

$$f^+(\mathbf{r}) \approx \rho_{\text{LUMO}}(\mathbf{r}). \quad (15)$$

They can provide extra information in the cases where the Fukui functions could not be obtained due to technical difficulties: mainly convergence issues with the charged systems or meta-stability problems with the anions. The extra electron in meta-stable anions tends to leave the molecular system and its molecular orbital contributions mainly come from the very diffuse functions in the basis set. Methods artificially binding this electron [56, 57] and enabling the calculation of $f^+(\mathbf{r})$ through Eq. 13 have been proposed, but have, however, not been applied in this study.

We will start with a discussion of the PbCl₂ molecule, for which the molecular plane is depicted in Fig. 1. The plots are all constructed analogously: the red lines indicate positive values, the blue dotted lines the negative ones, whereas the bold, black line represents the zero-contour. The exact contour values are given in the figure caption. A general look at any of the plots immediately shows that the inclusion of relativistic effects is vital for obtaining quantitatively correct Fukui functions since the variations induced by these effects are of the same order of magnitude as the non-relativistic functions themselves. It is also noticeable that any of the methodologies used, be it a scalar relativistic, a spin-orbit relativistic, or even an ECP approach, already take the largest portion of the effects into account. There are, however, some differences between the various levels of theory; especially the presence of the spin-orbit coupling contribution appears significant to get highly accurate results for PbCl₂ with respect to the four-component reference. Analysing the electrophilic Fukui function $f^-(\mathbf{r})$ and the density $\rho_{\text{HOMO}}(\mathbf{r})$ shows that the scalar ZORA and pseudopotential approach present the same features, but that the inclusion of spin-orbit coupling effects introduces some extra variations. Even so, they are mainly restricted to the core regions. The scalar ZORA and the ECP calculations for the nucleophilic Fukui function $f^+(\mathbf{r})$ and the LUMO density only induce changes in the core regions, whereas the spin-orbit ZORA and four-component calculations provoke significant variations in the valence region as well. The LUMO density presents a nodal plane for the non-relativistic and scalar relativistic calculations as it results from a linear combination of the chlorine 3p_x and lead 6p_x atomic orbitals, where the x axis is by convention taken as perpendicular to the molecular plane, and thus belongs to the b₁ irreducible representation. Inclusion of spin-orbit coupling effects requires the use of double group symmetry for the construction of the molecular spinors, which explains the disappearance of

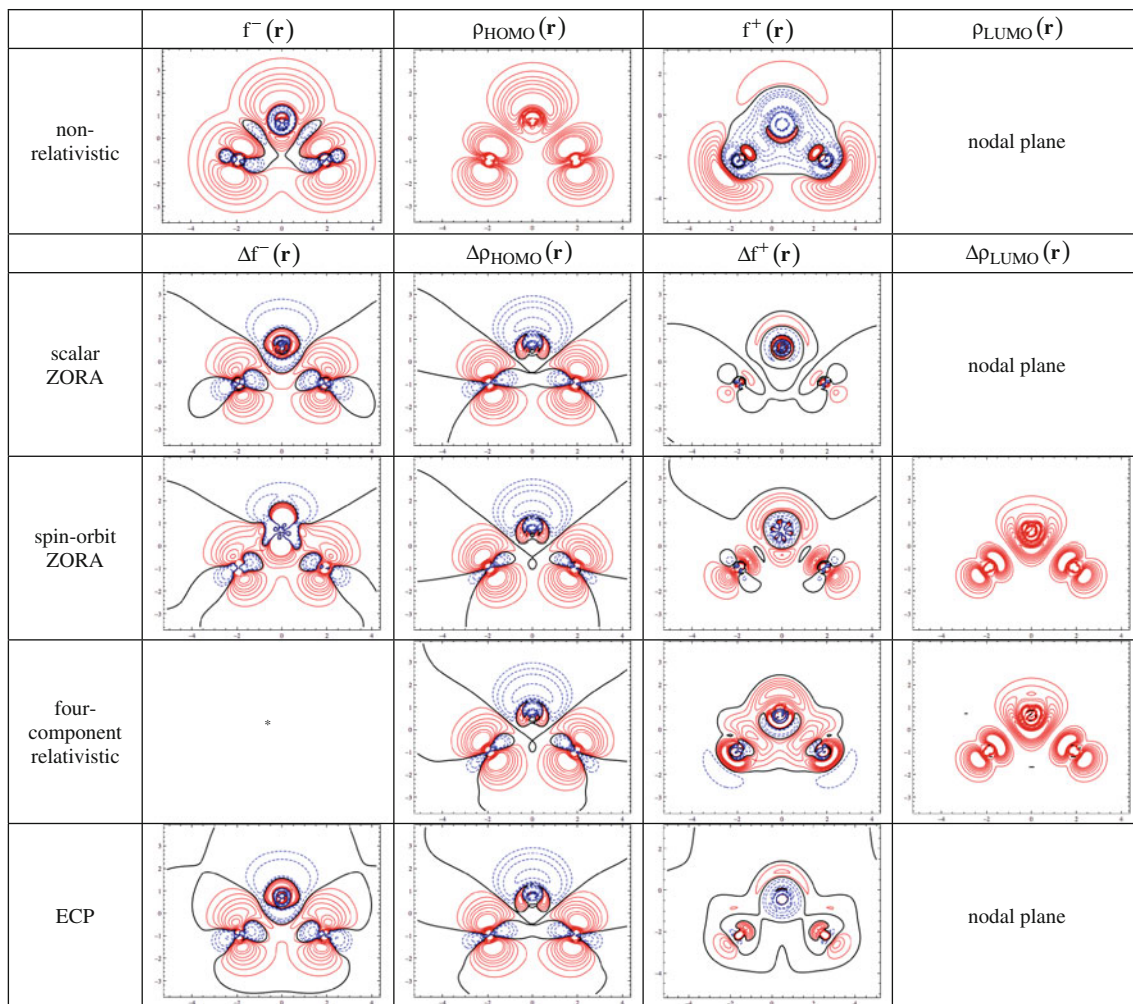


Fig. 1 This figure shows contour plots of the non-relativistic Fukui functions $f^\pm(\mathbf{r})$ and the frontier orbital/spinor densities $\rho_{\text{HOMO/LUMO}}(\mathbf{r})$ and difference plots of their relativistic counterparts as compared to the non-relativistic cases for the PbCl_2 molecule. The molecular plane is depicted with the Pb atom at the (0, 0, 0.6) coordinate (in Å). The red contour lines indicate positive values, the blue dotted lines the negative ones, whereas the bold, black line

represents the zero-contour. The contour values for $f^-(\mathbf{r})$, $\Delta f^-(\mathbf{r})$, $\rho_{\text{HOMO}}(\mathbf{r})$, and $\Delta \rho_{\text{HOMO}}(\mathbf{r})$ equal, in a.u., -0.0050 , -0.0020 , -0.0010 , -0.0005 , 0.0000 , 0.0002 , 0.0006 , 0.0012 , 0.0020 , 0.0030 , 0.0050 , and 0.0070 , while these of $f^+(\mathbf{r})$, $\Delta f^+(\mathbf{r})$, $\rho_{\text{LUMO}}(\mathbf{r})$, and $\Delta \rho_{\text{LUMO}}(\mathbf{r})$ are given by -0.0020 , -0.0015 , -0.0010 , -0.0005 , 0.0000 , 0.0002 , 0.0004 , 0.0006 , 0.0008 , 0.0010 , 0.0012 , 0.0014 , and 0.0016 . Asterisk indicates SCF convergence problem

the nodal plane in the spin-orbit ZORA and four-component plots.

Instead of showing all the obtained results, as we did for PbCl_2 , we will now only focus on the most relevant ones for the discussion of Bi_2H_4 , for which plots in the molecular symmetry plane are given in Fig. 2. The $f^+(\mathbf{r})$ plots have been left out as some of the calculations converged to unbound anionic states which gives rise to non-representative nucleophilic Fukui functions. The scalar relativistic effects are equally well described by the ECP calculations and by the scalar ZORA approach. These scalar relativistic methodologies reproduce most of the relativistic changes, when comparing their results with the four-component reference ones. Spin-orbit coupling effects induce some minor variations, which are mainly localised at the Bi

nuclei and in the Bi–Bi bonding region. These observations are in line with the ones made for the electrophilic Fukui function and the LUMO density of PbCl_2 .

For the last molecule to be studied, $(\text{CH}_3)_2\text{SAuCl}$, whose molecular symmetry plane is represented in Fig. 3, the $f^+(\mathbf{r})$ results are omitted because the anions have been found to be meta-stable with respect to electron auto-detachment [58], as indicated by electron affinity values of the order of -0.2 eV, for all levels of theory. Since the molecular symmetry plane forms a nodal plane of the LUMO, only the $f^-(\mathbf{r})$ and $\rho_{\text{HOMO}}(\mathbf{r})$ data are shown. In this case some minor deviations in the HOMO density can be observed between the ECP and the scalar ZORA calculations, especially at the chlorine end of the molecule, while the Fukui function $f^-(\mathbf{r})$ does not seem to suffer from

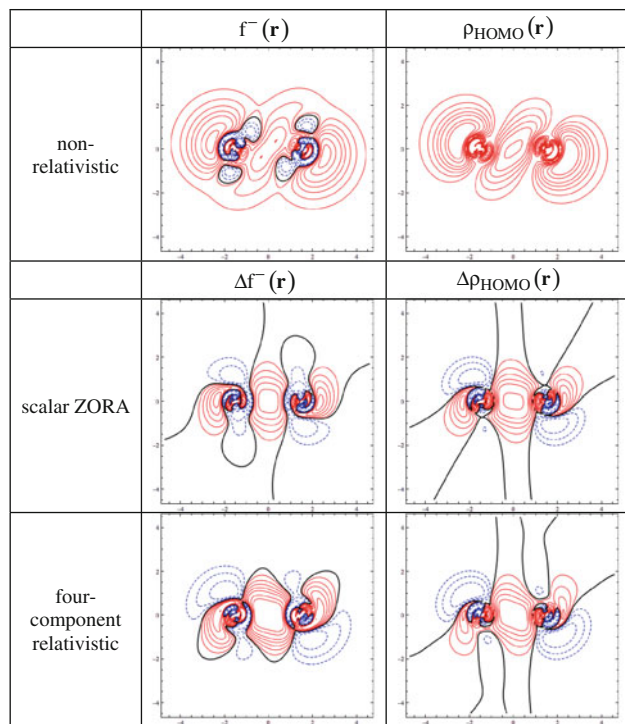


Fig. 2 Contour and difference plots for Bi_2H_4 . The molecular symmetry plane is depicted with the Bi nuclei at the $(-1.5, 0.0)$ and $(1.5, 0.0)$ coordinates (in Å). The contour specifications are identical to those in Fig. 1

this. Although well-converged results for the spin-orbit relativistic ZORA and four-component calculations could not be obtained for the cationic system, we are quite confident that the scalar ZORA approach encompasses almost all of the relativistic effects. This is because of the resemblance of their HOMO densities and the fact that spin-orbit coupling effects are more important for heavy *p*-block elements than for the transition metal ones.

To summarise this quantitative analysis, the Fukui functions, as well as the frontier orbital densities, improve significantly when relativistic effects are included. The scalar relativistic effects seem to provide the largest contribution and are almost equally well described by the scalar ZORA and the pseudopotential approach. Some disadvantages of ECPs [59–61] have, however, been discussed in previous studies concerning the relativistic effects on the electron density, but since these issues mainly focus on a very accurate description of the atomic core regions and shell structure they are of less relevance to the Fukui functions, which are to be accurately known in the valence region, where the chemical interactions occur. The inclusion of spin-orbit coupling contributions slightly improves the results when compared to the four-component reference, especially for the heavy *p*-block compounds.

In the last part of this section, we will focus on the qualitative changes the Fukui functions undergo and how

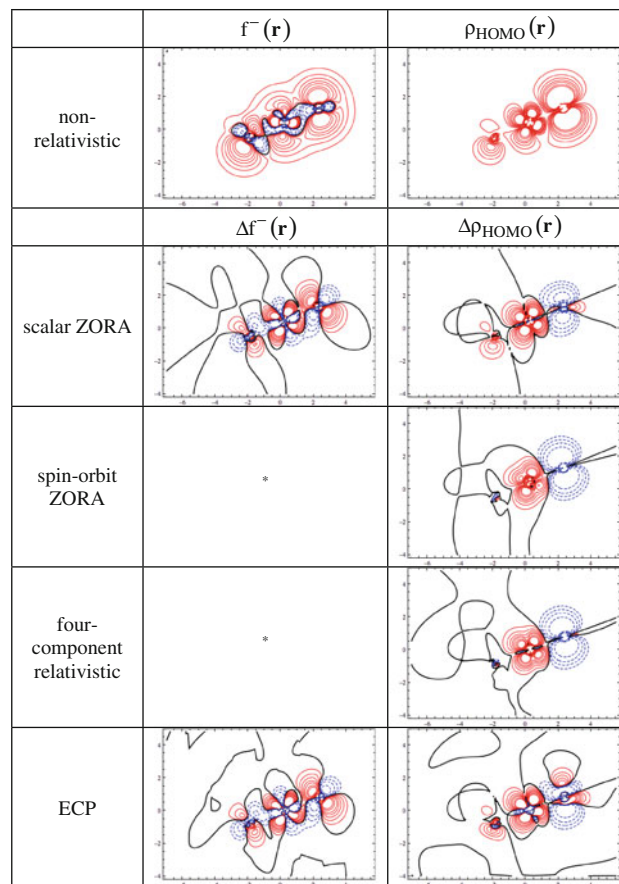


Fig. 3 Contour and difference plots for $(\text{CH}_3)_2\text{SAuCl}$. The molecular symmetry plane is depicted with the Au nucleus at the $(0.3, 0.0)$ coordinates and the Cl nucleus at the $(2.4, 0.8)$ coordinates (in Å). The contour specifications are identical to those in Fig. 1. Asterisk indicates SCF convergence problem

these affect the reactivity description. A chemical interpretation is most easily done by mapping the Fukui function on the Van der Waals surface (represented here by an iso-density surface with density values of 0.002 a.u. [62]). Figure 4 shows such plots for the Fukui function $f^-(\mathbf{r})$, describing where electrophilic attacks will preferably take place, for the studied molecules. The relativistic Fukui function, obtained by the most relevant relativistic approach, as specified in the figure caption, is compared with the non-relativistic result. The colour scale is chosen in such a way that red indicates regions of poor reactivity towards electrophilic attacks, whereas blue corresponds to highly reactive zones. It is important to note that the quantitative features described above are translated into clear, qualitative differences. In all three molecules, the reactivity of the heavy element towards electrophilic attacks decreases when relativistic corrections are taken into account. Despite the significance of the changes, the reactivity order of the various atoms does not appear to change for Bi_2H_4 and $(\text{CH}_3)_2\text{SAuCl}$. The situation of

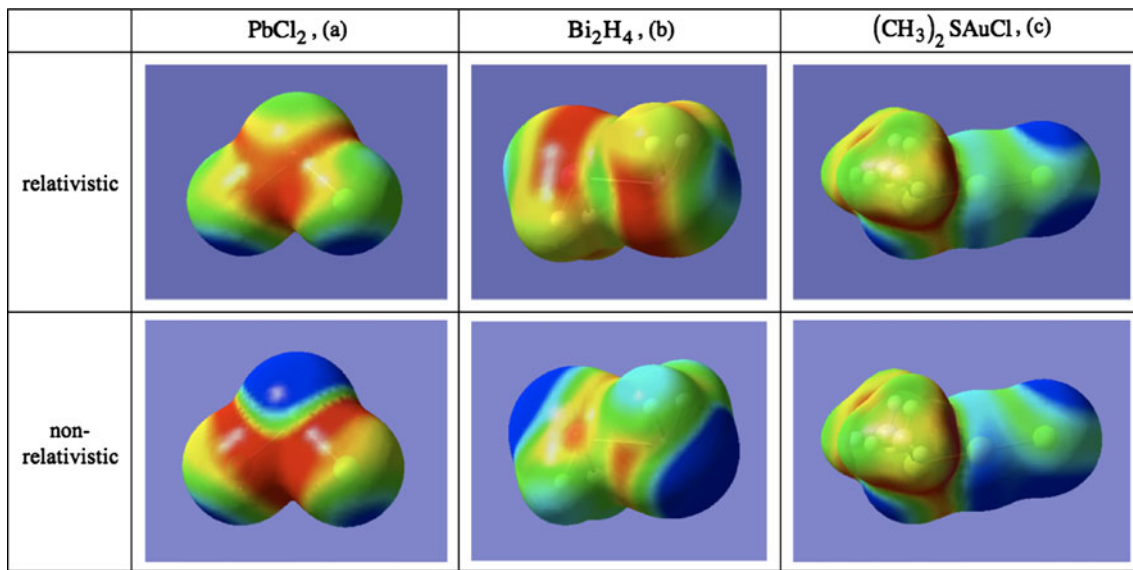


Fig. 4 The Fukui function $f^-(r)$ mapped on the Van der Waals surface. The relativistic results have been obtained with the spin-orbit relativistic ZORA approach for PbCl_2 , the four-component methodology for Bi_2H_4 and the scalar relativistic ZORA approximation for $(\text{CH}_3)_2\text{SAuCl}$. The colour scales are chosen in such a way that red

[$f^-(\mathbf{r})$ values not higher than 3.0×10^{-4} a.u. for (a) and 1.0×10^{-4} a.u. for (b) and (c)] indicates regions of poor reactivity towards electrophilic attacks, whereas blue [$f^-(\mathbf{r})$ values not lower than 7.0×10^{-4} a.u. for (a) and 6.0×10^{-4} a.u. for (b) and (c)] corresponds to highly reactive zones

PbCl_2 , on the other hand, is remarkable: while the non-relativistic Fukui function $f^-(\mathbf{r})$ predicts the lead atom to be the preferred reactive site for electrophilic attacks, the relativistic result excludes this site to the benefit of the chlorine centres. This relativistic behaviour is in agreement with the typical reactions PbCl_2 is involved in [22]. The presented results all indicate that the inclusion of relativistic effects in the analysis of the Fukui functions of heavy-element compounds is indispensable, a conclusion which can, in principle, be extended to the other local and global reactivity indices of conceptual DFT.

5 Conclusion

The aim of the paper was to acquire a deeper insight into the importance of relativistic effects on local reactivity indices as defined within conceptual DFT by analysing a set of three benchmark heavy-element molecules. The Fukui functions, which are the primary descriptors so far as local electrophilic and nucleophilic reactivity is concerned, and the frontier molecular orbital densities have been calculated with various (quasi-)relativistic approaches. The inclusion of relativistic effects by any of the methodologies has been shown to provide a significant improvement to the non-relativistic functions, not only in a quantitative sense, as the qualitative reactivity picture changes as well. Scalar relativistic effects are almost equally well described by scalar ZORA and ECP calculations. Standard scalar relativistic low-order Douglas-Kroll-Hess theory, which has

not been used in this study, can be expected to provide comparable results. Spin-orbit coupling effects, as taken into account by spin-orbit relativistic ZORA or four-component calculations, add minor variations. The four-component methodology, which is still complicated to use on a routine basis due to its extensive computational requirements, can be bypassed by one of the quasi-relativistic approaches without losing essential reactivity information.

Acknowledgments N.S. acknowledges the Research Foundation, Flanders (FWO) for a position as research assistant and a research stay at M. Reiher's group at the ETH Zurich. F.D.P. and P.G. thank the Vrije Universiteit Brussel (VUB) and FWO for continuous support to their research group. R.M. and M.R. gratefully acknowledge financial support by the Swiss National Science Foundation SNF (project 200020-121870).

Note added in Proof After having revised this paper we got aware of a recent paper that investigates relativistic effects on the Fukui function of gold clusters: De HS, Krishnamurti S, Pal S (2009) J Phys Chem C 113:7101–7106.

References

1. Parr RG, Yang W (1989) Density functional theory of atoms and molecules. Oxford University Press, New York
2. Chermette H (1999) J Comp Chem 20:129–154
3. Geerlings P, De Proft F, Langenaeker W (2003) Chem Rev 103:1793–1873
4. Ayers PW, Anderson JSM, Bartolotti LJ (2005) Int J Quantum Chem 101:520–534

5. Chattaraj PK, Sarkar U, Roy DR (2006) *Chem Rev* 106:2065–2091
6. Geerlings P, De Proft F (2008) *Phys Chem Chem Phys* 10:3028–3042
7. Hinze J, Jaffé HH (1962) *J Am Chem Soc* 84:540–546
8. Hinze J, Jaffé HH (1963) *Can J Chem* 41:1315–1328
9. Hinze J, Jaffé HH (1963) *J Phys Chem* 67:1501–1506
10. Hinze J, Whitehead MA, Jaffé HH (1963) *J Am Chem Soc* 85:148–154
11. Bergmann D, Hinze J (1987) *Struct Bonding* 66:145–190
12. Bergmann D, Hinze J (1996) *Angew Chem Int Ed* 35:781–781
13. Pearson RG (1963) *J Am Chem Soc* 85:3533–3539
14. Pearson RG (1966) *Science* 151:172–177
15. Pearson RG (1997) *Chemical hardness*. Wiley, New-York
16. Fukui K, Yonezawa T, Shingu H (1952) *J Chem Phys* 20:722–725
17. Fukui K (1982) *Science* 218:747–754
18. Parr RG, Donnelly RA, Levy M, Palke WE (1978) *J Chem Phys* 68:3801–3807
19. Ayers PW, Levy M (2000) *Theor Chem Acc* 103:353–360
20. Parr RG, Pearson RG (1983) *J Am Chem Soc* 105:7512–7516
21. Parr RG, Yang WT (1984) *J Am Chem Soc* 106:4049–4050
22. Elschenbroich C (2006) *Organometallics*. Wiley, Weinheim
23. Giju KT, De Proft F, Geerlings P (2005) *J Phys Chem A* 109:2925–2936
24. Perdew JP, Parr RG, Levy M, Balduz JL (1982) *Phys Rev Lett* 49:1691–1694
25. Kohn W, Sham LJ (1965) *Phys Rev A* 140:1133–1138
26. Rajagopal AK, Callaway J (1973) *Phys Rev B* 7:1912–1919
27. Saue T, Helgaker T (2002) *J Comput Chem* 23:814–823
28. Engel E, Dreizler RM (1996) *Top Curr Chem* 181:1–80
29. Reiher M, Hinze J (2003) In: Hess BA (ed) *Relativistic effects in heavy-element chemistry and physics*. Wiley, Weinheim
30. Reiher M, Wolf A (2009) *Relativistic quantum chemistry*. Wiley, Weinheim
31. Foldy LL, Wouthuysen SA (1950) *Phys Rev* 78:29–36
32. Douglas M, Kroll NM (1974) *Ann Phys* 82:89–155
33. Hess BA (1986) *Phys Rev A* 33:3742–3748
34. Reiher M (2006) *Theor Chem Acc* 116:241–252
35. Chang C, Pelissier M, Durand P (1986) *Phys Scr* 34:394–404
36. van Lenthe E, Baerends EJ, Snijders JG (1993) *J Chem Phys* 99:4597–4610
37. van Lenthe E, Baerends EJ, Snijders JG (1994) *J Chem Phys* 101:9783–9792
38. Dolg M (2000) In: Grotendorst J (ed) *Modern methods and algorithms of quantum chemistry*. John von Neumann Institute for Computing, Jülich
39. Dolg M (2002) In: Schwerdtfeger P (ed) *Relativistic quantum chemistry—part 1 fundamentals*. Elsevier, Amsterdam
40. Michalak A, De Proft F, Geerlings P, Nalewajski RF (1999) *J Phys Chem A* 103:762–771
41. Ayers PW, De Proft F, Borgoo A, Geerlings P (2007) *J Chem Phys* 126:224107
42. Sablon N, De Proft F, Geerlings P (2009) *J Chem Theory Comput* 5:1245–1253
43. Flores-Moreno R, Melin J, Ortiz JV, Merino G (2008) *J Chem Phys* 129:224105
44. Ayers PW, Melin J (2007) *Theor Chem Acc* 117:371–381
45. Eickerling G, Mastalerz R, Herz V, Scherer W, Himmel HJ, Reiher M (2007) *J Chem Theory Comput* 3:2182–2197
46. Becke AD (1988) *Phys Rev A* 38:3098–3100
47. Perdew JP (1986) *Phys Rev B* 33:8822–8824
48. ADF2006.01, SCM, Theoretical chemistry. Vrije Universiteit, Amsterdam, The Netherlands
49. Jensen HJ, Saue T, Visscher L with contributions from Bakken V, Eliav E, Enevoldsen T, Fleig T, Fossgaard O, Helgaker T, Laerdahl J, Larsen CV, Norman P, Olsen J, Pernpointner M, Pedersen JK, Ruud K, Salek P, van Stralen JNP, Thyssen J, Visser O, Winther T (2004) Dirac, a relativistic ab initio electronic structure program, Release DIRAC04.0
50. Dyall KG (2004) *Theor Chem Acc* 112:403–409
51. Dyall KG (2002) *Theor Chem Acc* 108:335–340
52. Dunning TH (1989) *J Chem Phys* 90:1007–1023
53. Frisch MJ, Trucks GW, Schlegel HB, Scuseria GE, Robb MA, Cheeseman JR, Montgomery JA Jr, Vreven T, Kudin KN, Burant JC, Millam JM, Iyengar SS, Tomasi J, Barone V, Mennucci B, Cossi M, Scalmani G, Rega N, Petersson GA, Nakatsuji H, Hada M, Ehara M, Toyota K, Fukuda R, Hasegawa J, Ishida M, Nakajima T, Honda Y, Kitao O, Nakai H, Klene M, Li X, Kno JE, Hratchian HP, Cross JB, Bakken V, Adamo C, Jaramillo J, Gomperts R, Stratmann RE, Yazyev O, Austin AJ, Cammi R, Pomelli C, Ochterski JW, Ayala PY, Morokuma K, Voth GA, Salvador P, Dannenberg JJ, Zakrzewski VG, Dapprich S, Daniels AD, Strain MC, Farkas O, Malick DK, Rabuck AD, Raghavachari K, Foresman JB, Ortiz JV, Cui Q, Baboul AG, Clifford S, Cioslowski J, Stefanov BB, Liu G, Liashenko A, Piskorz P, Komaromi I, Martin RL, Fox DJ, Keith T, Al-Laham MA, Peng CY, Nanayakkara A, Challacombe M, Gill PMW, Johnson B, Chen W, Wong MW, Gonzalez C, Pople JA (2005) Gaussian 03, Revision D.01. Gaussian, Inc, Wallingford
54. Metz B, Stoll H, Dolg M (2000) *J Chem Phys* 113:2563–2569
55. Figgen D, Rauhut G, Dolg M, Stoll H (2005) *Chem Phys* 311:227–244
56. Tozer DJ, De Proft F (2007) *J Chem Phys* 127:7
57. Sablon N, De Proft F, Geerlings P, Tozer DJ (2007) *Phys Chem Chem Phys* 9:5880–5884
58. Tozer DJ, De Proft F (2005) *J Phys Chem A* 109:8923–8929
59. Kohout M, Savin A, Preuss H (1991) *J Chem Phys* 95:1928–1942
60. Hebben N, Himmel HJ, Eickerling G, Herrmann C, Reiher M, Herz V, Presnitz M, Scherer W (2007) *Chem Eur J* 13:10078–10087
61. Eickerling G, Reiher M (2008) *J Chem Theory Comput* 4:286–296
62. Purvis GD III (1991) *Comput Aided Mol Des* 5:55–80